A priori error estimation of the structure-preserving modal model reduction by state residualization of a grid forming converter for use in 100% power electronics transmission systems

Quentin Cossart, Frédéric Colas, Xavier Kestelyn

A priori error estimation of the structure-preserving modal model reduction by state residualization of a grid forming converter for use in 100% power electronics transmission systems

Q.Cossart*, F.Colas*, X.Kestelyn*,

**Univ. Lille, Arts et Metiers ParisTech, Centrale Lille, HEI,*
EA 2697-L2EP-Laboratoire d'Electrotechnique et d'Electronique de Puissance, F-59000 Lille, France,
quentin.cossart@ensam.eu

Keywords: Model Order Reduction, Simulation, Power System, Power Electronics.

Abstract

This article deals with the model order reduction by state residualization of power electronic converters. It presents a method to a priori estimate the error induced by this reduction. This method helps choosing the most suitable reduced model, the one that minimizes the error, depending on the simulated events. When applied to a system with several converters, it helps choosing which converter to reduce and how much, in order to simplify the models while keeping a sufficient accuracy.

1 Introduction

The development of renewable energies and High Voltage Direct Current (HVDC) links rapidly increase the Power Electronics (PE) penetration in the transmission grids. This makes the study of all-converter-interfaced power systems (see Figure 1) necessary [1].

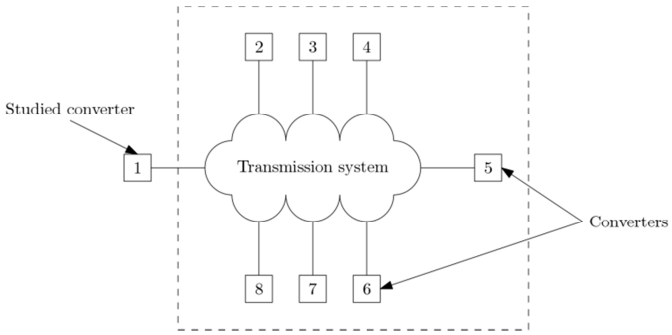

Figure 1: Structure of a 100% PE power system.

Because of the systems size and the converters complexity, numerical simulations are needed. Converters are physically different from synchronous generators. Therefore, commonly used tools, like the phasor approximation, might not be relevant. Usually, simulations of PE systems are based on detailed EMT [2] models but, in the case of large systems, the computation time would be large and the analysis complicated.

Consequently, Model Order Reduction (MOR) methods can be useful [3], to simplify the models while keeping a good accuracy. Several methods exist [4]. Yet most of them use basis changes and truncations, altering the system's structure and changing its state variables. This is why a MOR by state residualization [4] is applied in this paper to the converters, in order to preserve their physical structure and state variables. It is indeed necessary in power systems stability studies to keep the structure and variables, in order to know which quantities are critical.

This paper presents a method to a priori estimate the error induced by this MOR in order to help the user choose the most suitable models, those that minimize this error, depending on the case study under consideration.

The first part of this paper presents the structure of the studied converter and its MOR. The second part deals with the method to a priori estimate the induced error and its application to find the most suitable reduced models in two test cases: one converter connected to the infinite grid and two converters connected to each other, a load and the infinite grid.

2 Structure-preserving model order reduction of a PE converter

In this part an example of PE converter is presented and reduced using the developed structure-preserving MOR method by state residualization. The first subsection presents the converter's structure and model while the second one introduces the MOR methodology.

2.1 Structure of the studied converter

Figure 2 presents the structure of the studied converter. The control is made of a classical cascaded loops structure with a current loop, a voltage loop and an external loop (here an active power and a reactive power droop controls). The power part is made of the DC/AC converter (the DC part is modelled with an ideal DC voltage source and the model for the converter is an averaged one), an RLC filter and a transformer modelled with an RL line. The aim of this grid forming converter is to generate the voltage at the PCC (Point of Common Coupling) v_o.

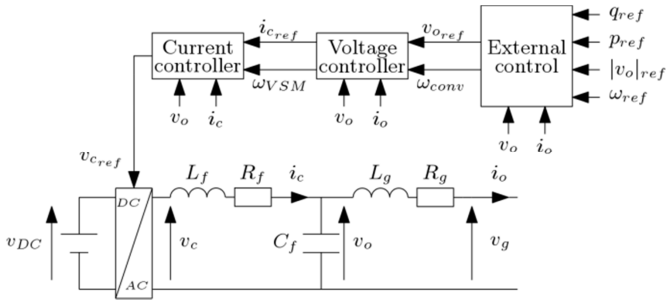

Figure 2: Structure of the studied converter.

The differential and algebraic equations describing this system and its control are given in Equations (1)-(31), starting from the external control (1)-(13), then the voltage control (14)-(17), the current control (18)-(21), the converter (22)-(23), the filter (24)-(27), the transformer (28)-(29) and the grid (30)-(31). The state variables are in red, the algebraic ones in blue, the parameters in green and the inputs in purple. The equations and parameters of the model are taken from [5] and more details can be found in this paper. The variables are expressed in the dq reference frame of the converter's frequency.

$$p_o = v_{o_d} i_{o_d} + v_{o_q} i_{o_q} \quad (1)$$

$$q_o = v_{o_q} i_{o_d} - v_{o_d} i_{o_q} \quad (2)$$

$$\frac{dp_m}{dt} + \omega_f p_m = \omega_f p_o \quad (3)$$

$$\frac{dq_m}{dt} + \omega_f q_m = \omega_f q_o \quad (4)$$

$$\frac{dM_{AD_d}}{dt} = \omega_{ff}\left(K_{FF} i_{o_d} - M_{AD_d}\right) \quad (5)$$

$$\frac{dM_{AD_q}}{dt} = \omega_{ff}\left(K_{FF} i_{o_q} - M_{AD_q}\right) \quad (6)$$

$$\Delta e_d = M_{AD_d} - K_{FF} i_{o_d} \quad (7)$$

$$\Delta e_q = M_{AD_q} - K_{FF} i_{o_q} \quad (8)$$

$$v_{o_{d_{ref}}} = |v_o|_{ref} + m_q\left(q_{ref} - q_m\right) + \Delta e_d \quad (9)$$

$$v_{o_{q_{ref}}} = \Delta e_q \quad (10)$$

$$\omega_{conv} = \omega_{ref} + m_p(p_{ref} - p_m) \quad (11)$$

$$\frac{1}{\omega_b}\frac{d\theta_{conv}}{dt} = \omega_{conv} \quad (12)$$

$$\Delta\theta = \theta_{conv} - \omega_g \omega_b t \quad (13)$$

$$\frac{d\xi_d}{dt} = K_{i_v}\left(v_{o_{d_{ref}}} - v_{o_d}\right) \quad (14)$$

$$\frac{d\xi_q}{dt} = K_{i_v}\left(v_{o_{q_{ref}}} - v_{o_q}\right) \quad (15)$$

$$i_{c_{d_{ref}}} = K_{FF_i} i_{o_d} + K_{p_v}\left(v_{o_{d_{ref}}} - v_{o_d}\right) - \ldots \quad (16)$$
$$\ldots\ \omega_{conv} C_f v_{o_q} + \xi_d$$

$$i_{c_{q_{ref}}} = K_{FF_i} i_{o_q} + K_{p_v}\left(v_{o_{q_{ref}}} - v_{o_q}\right) + \ldots \quad (17)$$
$$\ldots\ \omega_{conv} C_f v_{o_d} + \xi_q$$

$$\frac{d\sigma_d}{dt} = K_{i_i}\left(i_{c_{d_{ref}}} - i_{c_d}\right) \quad (18)$$

$$\frac{d\sigma_q}{dt} = K_{i_i}\left(i_{c_{q_{ref}}} - i_{c_q}\right) \quad (19)$$

$$v_{c_{d_{ref}}} = K_{FF_v} v_{o_d} + K_{p_i}\left(i_{c_{d_{ref}}} - i_{c_d}\right) - \ldots \quad (20)$$
$$\ldots\ \omega_{conv} L_f i_{c_q} + \sigma_d$$

$$v_{c_{q_{ref}}} = K_{FF_v} v_{o_q} + K_{p_i}\left(i_{c_{q_{ref}}} - i_{c_q}\right) + \ldots \quad (21)$$
$$\ldots\ \omega_{conv} L_f i_{c_d} + \sigma_q$$

$$v_{c_d} = v_{c_{d_{ref}}} \quad (22)$$

$$v_{c_q} = v_{c_{q_{ref}}} \quad (23)$$

$$\frac{L_f}{\omega_b}\frac{di_{c_d}}{dt} = v_{c_d} - v_{o_d} - R_f i_{c_d} + \omega_{conv} L_f i_{c_q} \quad (24)$$

$$\frac{L_f}{\omega_b}\frac{di_{c_q}}{dt} = v_{c_q} - v_{o_q} - R_f i_{c_q} - \omega_{conv} L_f i_{c_d} \quad (25)$$

$$\frac{C_f}{\omega_b}\frac{dv_{o_d}}{dt} = i_{c_d} - i_{o_d} + \omega_{conv} C_f v_{o_q} \quad (26)$$

$$\frac{C_f}{\omega_b}\frac{dv_{o_q}}{dt} = i_{c_q} - i_{o_q} - \omega_{conv} C_f v_{o_d} \quad (27)$$

$$\frac{L_g}{\omega_b}\frac{di_{o_d}}{dt} = v_{o_d} - v_{g_d} - R_g i_{o_d} + \omega_{conv} L_g i_{o_q} \quad (28)$$

$$\frac{L_g}{\omega_b}\frac{di_{o_q}}{dt} = v_{o_q} - v_{g_q} - R_g i_{o_q} - \omega_{conv} L_g i_{o_d} \quad (29)$$

$$v_{g_d} = \cos(\Delta\theta) v_{g_{d_g}} + \sin(\Delta\theta) v_{g_{q_g}} \quad (30)$$

$$v_{g_q} = -\sin(\Delta\theta) v_{g_{d_g}} + \cos(\Delta\theta) v_{g_{q_g}} \quad (31)$$

This system is made of 15 differential equations/variables. It is thus a 15th order nonlinear differential algebraic system. Table 1 and 2 give the values of the parameters and inputs.

ω_f	31.4 rad/s	R_g	0.01 pu	m_q	0.0001
ω_{ff}	16.66 rad/s	L_g	0.2 pu	K_{p_i}	0.74
ω_b	314 rad/s	K_{FF}	0.01	K_{p_v}	0.80
R_f	0.005 pu	K_{FF_i}	1	K_{i_i}	1.19
L_f	0.15 pu	K_{FF_v}	1	K_{i_v}	1.16
C_f	0.066 pu	m_p	0.02		

Table 1: Parameters.

$\|v_o\|_{ref}$	1 pu	p_{ref}	0.5 pu	$v_{g_{q_g}}$	0 pu
ω_{ref}	1 pu	q_{ref}	0 pu		
ω_g	1 pu	$v_{g_{d_g}}$	1 pu		

Table 2: Inputs.

To sum up, the converter is modelled by a 15th order nonlinear differential-algebraic model. The next subsection

investigates the MOR of this model, in order to facilitate the analysis and simulation of large transmission systems with several converters.

2.2 Model order reduction of the converter

Several MOR methods exist, like the balanced truncation [6], the proper orthogonal decomposition [4], the modal truncation [7] or Krylov methods [8]. However, these methods use basis changes and truncations (projections on subspaces), which change the physical structure of the system. The state variables are indeed altered by the MOR, which is not wanted here for analyses issues. It is indeed mandatory, for stability studies, to keep the variables in order to identify the critical ones.
This is why a method using state residualization [4] is investigated here. The state residualization consists in freezing the dynamics of some chosen states of the system. These states are thus changed into algebraic variables, which reduces the order of the system. For example, in the studied converter, the residualization of the state q_m consists in changing Equation (32) into (33).

$$\frac{dq_m}{dt} + \omega_f q_m = \omega_f q_o \quad (32)$$

$$0 + \omega_f q_m = \omega_f q_o \quad (33)$$

One advantage of doing state residualization is that it can easily be implemented in a program/language that solves differential-algebraic equations, like Modelica [9] (which is used here). This language consists in writing the differential and algebraic equations almost like in the natural language, like shows Figure 3, which is very convenient.

```
// Dynamic of the filter
Lf / wb * der(icd_g) = vcd_g - Rf * icd_g + wg * Lf * icq_g - vod_g;
Lf / wb * der(icq_g) = vcq_g - Rf * icq_g - wg * Lf * icd_g - voq_g;
Cf / wb * der(vod_g) = icd_g + wg * Cf * voq_g - iod_g;
Cf / wb * der(voq_g) = icq_g - wg * Cf * vod_g - ioq_g;
```

Figure 3: Modelling of the RLC filter in the Modelica language.

With the used reduction method, the variables are kept the same, and so is the structure of the system. To illustrate this; figures 4 and 5 show the evolution of the current controller when the MOR is applied (i.e. when the state variables of the PI controllers of the current control are residualized). During the process, Equations (18) and (19) are changed into Equations (34) and (35).

$$i_{c_{d_{ref}}} = i_{c_d} \quad (34)$$

$$i_{c_{q_{ref}}} = i_{c_q} \quad (35)$$

It can be seen on this figures that the reduced system can still be represented in a physical way, which is not the case with methods such as the POD or the balanced truncation (they indeed project the state variables on a subspace, which changes them).

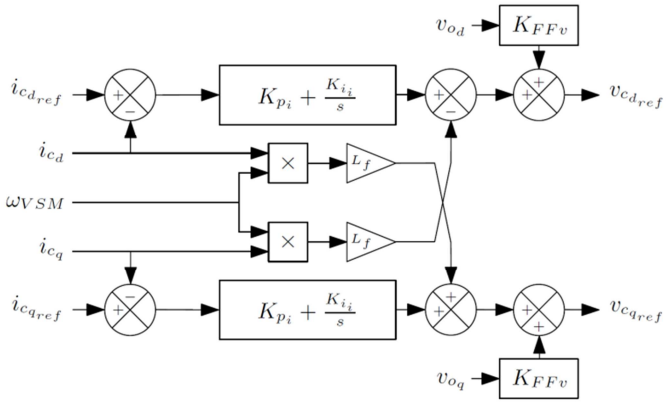

Figure 4: Structure of the current control.

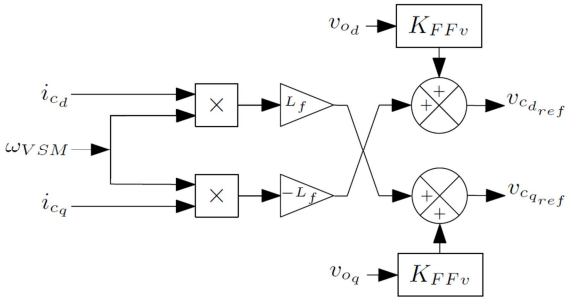

Figure 5: Structure of the current control after the MOR.

The philosophy of the method is then to find the states that can be residualized without too much decreasing the accuracy of the model. To do so, a modal approach using the participation factors is used. The participation factors give the dependencies between the states and the modes/poles of the linearized system. This way it is known which poles are discarded when some states are residualized. They are numbers between 0 and 1, and there is one for each state/pole couple. For each state, the sum of its participation factors in each pole is equal to 1. And for each pole, the sum of its participation factors in each state is equal to 1. To calculate the participation factors, the model first needs to be linearized around its operating point, which gives Equation (36) (the algebraic equations are injected in the differential ones), with $x = \left(v_{od}\ v_{oq}\ i_{od}\ i_{oq}\ i_{cd}\ i_{cq}\ q_m\ M_{AD_d}\ M_{AD_q}\ \xi_d\ \xi_q\ \theta_{conv}\ \sigma_d\ \sigma_q\ p_m\right)^t$.

$$\frac{d\Delta x}{dt} = \mathrm{A}\Delta x + \mathrm{B}\Delta u \quad (36)$$

Then the participation factor of Δx_i in λ_j, an eigenvalue of A, is given by Equation (37).

$$P_{i,j} = u_{i,j} y_{i,j} \quad (37)$$

In this equation $y_{i,j}$ is the j^{th} entry of the i^{th} normalized right eigenvector of A and $u_{i,j}$ is the j^{th} entry of the i^{th} normalized left eigenvector of A. Figure 6 gives an example for one eigenvalue. It shows that the considered eigenvalue is mainly linked to the dynamics of the variables $\sigma_d, \sigma_q, \xi_d, \xi_q$ and θ_{conv}.

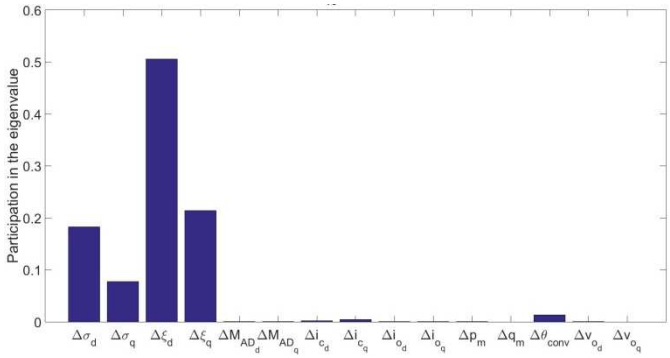

Figure 6: Participation of the states in the eigenvalue $\lambda_1 = -1.4$.

This process is done for each eigenvalue. The participation factors are ranked from the largest to the smallest and the first ones are chosen to have a total participation of at least 90%. It leads to Table 3. Note that each eigenvalue is linked to several states and each state participates in several eigenvalues (this is a coupled system). This leads to groups of eigenvalues/state variables.

Eigenvalues	State variables
$\lambda_{14,15} = -790 \pm 3821i$ $\lambda_{12,13} = -759.6 \pm 3331i$ $\lambda_{10,11} = -21 \pm 133.6i$	$v_{od}, v_{oq}, i_{od}, i_{oq}, i_{cd}, i_{cq}$
$\lambda_9 = -31.4$	q_m
$\lambda_8 = -17.2$ $\lambda_7 = -16.2$	M_{AD_d}, M_{AD_q}
$\lambda_{5,6} = -15.5 \pm 28.3i$ $\lambda_4 = -1.7$ $\lambda_{2,3} = -1.5 \pm 0.1i$ $\lambda_1 = -1.4$	$\xi_d, \xi_q, \theta_{conv}, \sigma_d, \sigma_q, p_m$

Table 3: Dependencies between the eigenvalues and the state variables of the system.

Thanks to Table 3, it is possible to know which dynamics to freeze in the nonlinear model in order to discard some poles in the linearized one while maintaining the other untouched. This method ensures the stability as the remaining are not moved (see Figure 7, where the fastest poles (i.e. the one with the largest negative real part) are removed for each reduced model. We can see that the remaining poles are really close to the initial ones.).

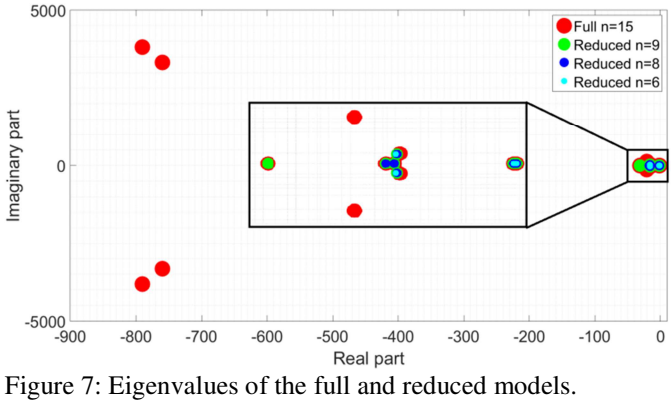

Figure 7: Eigenvalues of the full and reduced models.

The question now is how to choose which poles to delete. Usually, the fastest ones (with the highest real part in absolute value) are removed [10] as they are linked to fast transients that are quickly cleared and they don't have any impact on the stability, which is not the case for the poles close to the imaginary axis. But there is no mathematical proof that this is the best solution in terms of accuracy. This is why the next section presents a method that estimates the error induced by the residualization and thus helps the user choose the most suitable reduced model for its studies (i.e. the best poles to keep/discard).

3 A priori estimation of the error induced by the reduction

This section presents the method to a priori estimate the error made by the MOR and the deduced optimization problem that helps minimizing it in order to have the most accurate reduced model. Two test cases with respectively one and two converters are then studied.

3.1 Mathematical method

To simplify, the linearized model is considered in Equation (38) (to simplify the writing, the Δ are removed).

$$\frac{dx}{dt} = \mathrm{A}x + \mathrm{B}u \tag{38}$$

The residualization consists in multiplying the first term of this equation by a diagonal matrix E, that has the same size as A, made of 1 and 0. If $E(i,i) = 0$, it means that the state x_i is residualized, if it is equal to 1, the state dynamic is kept. The trace of E gives the order of the reduced model. Table 3 gives some constraints on E in order to keep the remaining poles unchanged. For example $\xi_d, \xi_q, \theta_{conv}, \sigma_d, \sigma_q$ and p_m must be kept (or residualized) together in order to properly remove the poles. The reduced model is then given in Equation (39).

$$E\frac{dx_r}{dt} = \mathrm{A}x_r + \mathrm{B}u \tag{39}$$

A Laplace transform give Equations (40) and (41).

$$X = (\mathrm{sI} - \mathrm{A})^{-1}\mathrm{B}U \tag{40}$$

$$X_r = (\mathrm{sE} - \mathrm{A})^{-1}\mathrm{B}U \tag{41}$$

Then a subtraction gives Equation (42).

$$X - X_r = [(\mathrm{sI} - \mathrm{A})^{-1} - (\mathrm{sE} - \mathrm{A})^{-1}]\mathrm{B}U = \varepsilon U \tag{42}$$

ε is the transfer function of the error induced by the MOR. It is a matrix of dimension $n \times p$ with $n \times n$ the size of A and $n \times p$ the size of B.

It is possible to choose the best E to minimize the maximum of the transfer function $\varepsilon(i,j)$ which represents the error for the i^{th} state variable when considering the j^{th} input. This optimization is summed up in Equations (43)-(44). In Equation 44, the constraints imposed by Table 3 are put in equation.

$$\text{minimize}_E\{\max_s(\varepsilon(i,j))\} \quad (43)$$

$$\begin{gathered} subject\ to: \\ E = diag(\delta_i), \delta_i \in \{0;1\}\ \forall i; \\ E(1,1) = E(2,2) = \cdots = E(5,5) = E(6,6); \\ E(8,8) = E(9,9); \\ E(10,10) = E(11,11) = \cdots = E(14,14) = E(15,15) \end{gathered} \quad (44)$$

This way it is possible to have a specific reduced model for each event to be simulated (each j), depending on the state variable that is looked at (each i).
Examples to illustrate this will be shown in the two next parts.

3.2 Application to find the best reduced model on a single converter test case

The first example is the converter of Figure 2 connected to an infinite grid. The considered state variable is the current in the converter i_{c_d} (the same results apply for i_{c_q}) and the considered input is the grid voltage $v_{g_{d_g}}$. Table 4 gives, for each specified size, the dynamics to freeze/the poles to discard in order to have the most accurate reduced model. These results are obtained by solving the optimization problem of Equations (43)-(44)

Model order	Frozen dynamics	Discarded poles
15	NA	NA
14	q_m	λ_9
13	M_{AD_d}, M_{AD_q}	λ_7, λ_8
12	M_{AD_d}, M_{AD_q}, q_m	$\lambda_7, \lambda_8, \lambda_9$
9	$v_{od}, v_{oq}, i_{od}, i_{oq}, i_{cd}, i_{cq}$	$\lambda_{10,11}, \lambda_{12,13}, \lambda_{14,15}$
8	$v_{od}, v_{oq}, i_{od}, i_{oq}, i_{cd}, i_{cq}, q_m$	$\lambda_{10,11}, \lambda_{12,13}, \lambda_{14,15}, \lambda_9$
7	$v_{od}, v_{oq}, i_{od}, i_{oq}, i_{cd}, i_{cq}, M_{AD_d}, M_{AD_q}$	$\lambda_{10,11}, \lambda_{12,13}, \lambda_{14,15}, \lambda_7, \lambda_8$
6	$v_{od}, v_{oq}, i_{od}, i_{oq}, i_{cd}, i_{cq}, M_{AD_d}, M_{AD_q}, q_m$	$\lambda_{10,11}, \lambda_{12,13}, \lambda_{14,15}, \lambda_7, \lambda_8, \lambda_9$

Table 4: Dynamics to freeze/ poles to discard for each reduced model size.

However, in this case, there is most of the time only one possible reduced model that respects Table 3 for a given size. This is why a more complex case with two converters is investigated in the next section. In this case, for each size, there are several possibilities for the reduced model, and the method helps choosing the best one.

3.3 Application to find the best reduced model on a two-converter test case

The system shown in figure 8 is considered. It is made of two identical converters, connected to each other and to a load and the infinite grid.

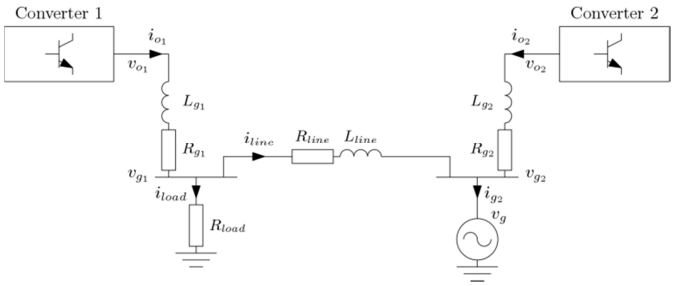

Figure 8: Considered 2-converter system.

The additional parameters are given in Table 5.

R_{line}	0.006 pu	L_{line}	0.2 pu	R_{load}	2 pu

Table 5: Additional parameters.

This case is more interesting than the previous one, as for each total size, different models are possible, as shows Table 6. This is the reason why the developed method is interesting here.

Total size	Converter 1/Converter 2 size
12	6/6
13	7/6 or 6/7
14	8/6 or 7/7 or 6/8
15	9/6 or 8/7 or 7/8 or 6/9
16	9/7 or 8/8 or 7/9
17	9/8 or 8/9
18	12/6 or 9/9 or 6/12
19	13/6 or 12/7 or 7/12 or 6/13
20	14/6 or 13/7 or 12/8 or 8/12 or 7/13 or 6/14
21	15/6 or 14/7 or 13/8 or 12/9 or 9/12 or 8/13 or 7/14 or 6/15
22	15/7 or 14/8 or 13/9 or 9/13 or 8/14 or 7/15
23	15/8 or 14/9 or 9/14 or 8/15
24	15/9 or 12/12 or 9/15
25	13/12 or 12/13
26	14/12 or 13/13 or 12/14
27	15/12 or 14/13 or 13/14 or 12/15
28	15/13 or 14/14 or 13/15
29	15/14 or 14/15

Table 6: Possible reduced models for each converter depending of the size of the whole system.

As an example, the considered state variable is the current in the first converter i_{cd1} (same for i_{cq1}) and the considered input is the load R_{load}. For the chosen total size of 21, figure 9 shows the estimated error for each possible combination in Table 6. It shows that to keep a good accuracy, converter 1 should not be reduced while converter 2 can.

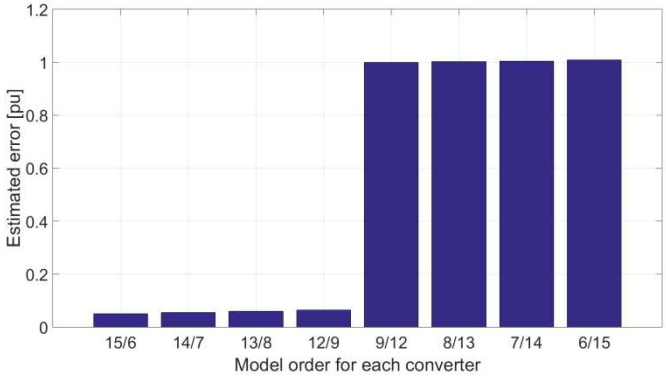

Figure 9: Estimated error for each combination

This helps choosing which converter to reduce and how much depending on the event and variable under consideration. On Figure 10, the evolution of the current in the first converter i_{c1} when R_{load} goes to 0 pu at 1s (short-circuit) and the fault is cleared after 100ms is shown for 3 cases: two full converters, a 15th order converter 1 and a 6th order converter 2, a 6th order converter 1 and a 15th order converter 2.

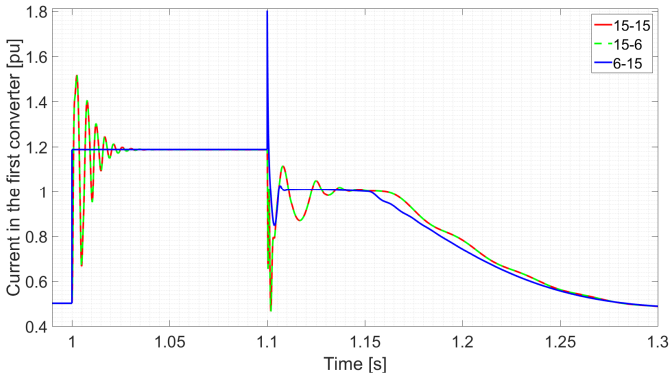

Figure 10: Evolution of the current in the three cases.

This figure shows that the case with a reduced first converter gives bad results during the short-circuit. It misses an overcurrent. On the other hand, it adds one that doesn't exist when the fault is cleared. The case with a reduced second converter gives results that are very close to the case with a full second converter. This is what was expected because the fault appears far from this converter and we are looking at the current in the first one. The developed method proved it. Moreover it can be used in cases where this conclusion is not obvious, where there are many converters in a large network.

4 Conclusion and perspectives

In this paper the MOR of PE systems is investigated. To keep the physical structure, a method by state residualization is used; and to ensure the stability, a method keeping the remaining poles of the system unchanged has been chosen. The main idea of this article is the development of a method that a priori estimates the error made by the reduced model and helps choosing the optimal one for each converter of the system depending on the event to be simulated and the variable to be looked at. A case with two converters has been tested. The method gives the best model for each converter. It now needs to be tested on systems with many converters. However, as it needs to enumerate all the possible combinations before finding the best one, the process is long. This is why a method to find the poles to eliminate more quickly is investigated at the moment.

Acknowledgements

This project has received funding from the European Union's Horizon 2020 research and innovation programme under grant agreement No 691800. This paper reflects only the authors' views and the European Commission is not responsible for any use that may be made of the information it contains.

References

[1] D. Ramasubramanian, Z. Yu, R. Ayyanar, V. Vittal, and J. M. Undrill, "Converter Model for Representing Converter Interfaced Generation in Large Scale Grid Simulations," *IEEE Trans. Power Syst.*, pp. 1–1, 2016.

[2] A. A. Van der Meer, M. Gibescu, M. Van der Meijden, W. L. Kling, and J. A. Ferreira, "Advanced Hybrid Transient Stability and EMT Simulation for VSC-HVDC Systems," *IEEE Trans. Power Deliv.*, vol. 30, no. 3, pp. 1057–1066, Jun. 2015.

[3] Y. Gu, N. Bottrell, and T. C. Green, "Reduced-Order Models for Representing Converters in Power System Studies," *IEEE Trans. Power Electron.*, pp. 1–1, 2017.

[4] A. C. Antoulas, *Approximation of Large-Scale Dynamical Systems*. Society for Industrial and Applied Mathematics, 2005.

[5] T. Qoria, F. Gruson, F. Colas, X. Guillaud, M.-S. Debry, and T. Prevost, "Tuning of cascaded controllers for robust grid-forming Voltage Source Converter," in *20th Power Systems Computation Conference, PSCC 2018*, 2018.

[6] A. Ramirez *et al.*, "Application of balanced realizations for model-order reduction of dynamic power system equivalents," *IEEE Trans. Power Deliv.*, vol. 31, no. 5, pp. 2304–2312, Oct. 2016.

[7] J. H. Chow, *Power system coherency and model reduction*. Springer, 2013.

[8] D. Chaniotis and M. A. Pai, "Model Reduction in Power Systems Using Krylov Subspace Methods," *IEEE Trans. Power Syst.*, vol. 20, no. 2, pp. 888–894, 2005.

[9] P. A. Fritzson, *Principles of object oriented modeling and simulation with Modelica 3.3 : a cyber-physical approach*. Wiley-IEEE Press, 2014.

[10] Q. Cossart, F. Colas, and X. Kestelyn, "Model reduction of converters for the analysis of 100% power electronics transmission systems," in *2018 IEEE International Conference on Industrial Technology (ICIT)*, 2018, pp. 1254–1259.